Bridging Scales: Explicit Forest Representation and Full-Physics LES for Improved Wind Resource Modelling

Journal of Physics: Conference Series **3232** (2026) 012010 doi:10.1088/1742-6596/3232/1/012010

Bridging Scales: Explicit Forest Representation and Full-Physics LES for Improved Wind Resource Modelling.

J.A. Sturm, P. van Dorp, A. Davidson

[1]Whiffle, Delft, The Netherlands
[2]Ørsted, Edinburgh, UK

E-mail: ardjan.sturm@whiffle.nl

Abstract. Sites with complex forestry and orography are challenging to model for wind resource assessment. Higher horizontal and vertical resolution, capturing the detailed physics requires precise implementation of the required physics and can lead to unrealistically high run times and thus prices. We propose a practical framework for adding those details in large eddy simulations, by adding multiple simulation nests, zooming in on the relevant sites to final horizontal resolution of 40m, while remaining connected to the synoptic weather. The costs are limited by the triple-nested high resolution domain, and a smart selection of representative days. The approach delivers time-series statistics of wind speed and turbulence intensity that capture key dependencies on wind direction, diurnal cycle, seasonality, height, and atmospheric stability. Cross-prediction errors between measurement devices are reduced from 6–12% with a traditional linear flow model to 3–5% with the proposed method.

1 Introduction

Forests remain one of the most persistent challenges in wind resource assessment modelling, especially in complex terrain. Their impact on wind flow and turbulence is highly heterogeneous, non-linear, and both time and scale-dependent, which makes flow simulations particularly challenging. In practice, forests are often represented in overly simplified forms. Canopy datasets are frequently sparse or restricted to very local scales, while atmospheric dynamics act on kilometer scales. At the same time, computational cost forces compromises between model resolution, long term representativity, and the convergence of performance metrics.

We propose a practical and scientifically rigorous framework for modelling forests in complex terrain. The region of interest is simulated with large eddy simulations (LES) at high resolution to resolve canopy and orography features from high-resolution input data. This fine-scale LES40 is embedded within a coarser LES100, with boundary conditions provided by a mesoscale model driven by ERA5 reanalysis data. Coarse-graining and global datasets ensure spatial continuity

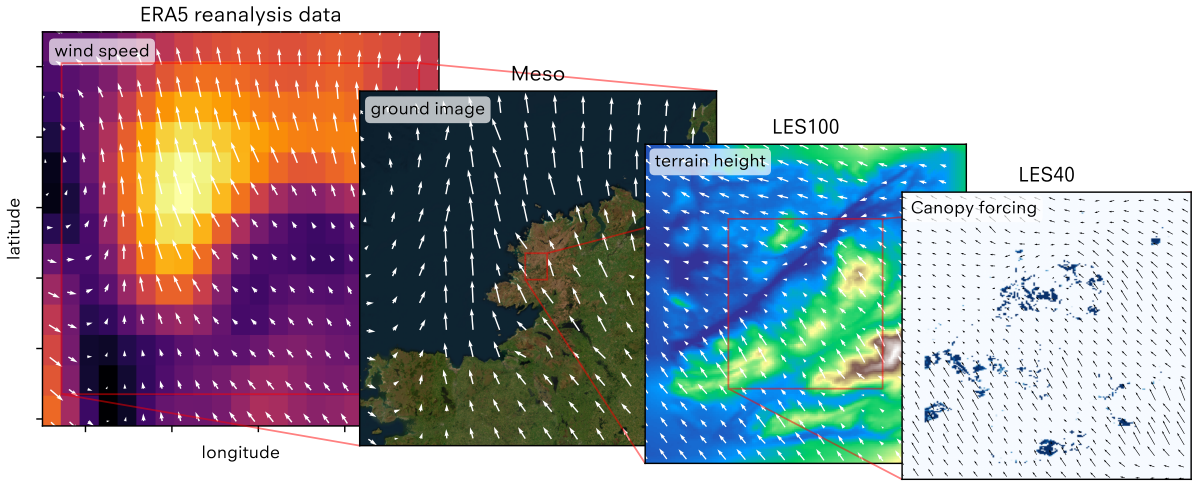

Figure 1: Example of the triple-nested setup at one of the validation sites, required to capture all relevant scales. ERA5 reanalysis data at 30 km resolution is used as input for the weather conditions on the domain boundary. The Meso model with a resolution of 2 km captures large scale weather phenomena, and improves orography and land sea masks from the ERA5 input. The LES model at 100 m resolution (LES100) resolves detailed orography and flow, which is then given as boundary conditions to a fine scale LES model at 40 m (LES40) resolution that includes tree canopies explicitly.

where detailed canopy data are unavailable. This nesting approach ensures that all relevant spatial scales are captured at a fidelity matching their importance for the local wind conditions. Unlike traditional flow modelling approaches such as linear flow models and Reynolds-averaged Navier–Stokes computational fluid dynamics (RANS-CFD), Whiffle LES models atmospheric conditions in a full-physics, time-varying manner. For example, seasonal and diurnal patterns in the wind conditions and atmospheric stability *emerge* from the real weather boundary conditions, the atmospheric radiation scheme and the interactive land surface scheme, instead of having to *prescribe* them as is the case in traditional models. Local wind conditions are fully represented in a cost-effective manner by a representative day selection routine based on uniform sampling of wind direction. The day selection routine enforces wind speed distributions and seasonality to match a specified (long-term) period, to provide representative wind-climate statistics.

In the context of this study, simulations were performed for 3 forested sites with substantial orographic complexity. The simulations are validated in terms of correlation in key metrics such as turbulence intensity, speed-up ratios between measurement locations, and diurnal and directional wind patterns observed between met masts. This framework provides industry with clear guidance on when high-resolution modelling of forests is worth the investment, balancing accuracy, long-term representativity, and computational cost.

2 Modeling recipe

2.1 Whiffle LES setup

Whiffle Large-Eddy Simulation (LES) resolves dominant turbulent motions while parameterizing subgrid-scale processes (1; 2; 3; 4; 5; 6). The model advances filtered 3D equations for momentum, temperature, and humidity, including a microphysics scheme for precipitation and a radiation scheme for solar and terrestrial fluxes. This allows the model to resolve buoy-

ancy effects associated with thermal, pressure or compositional stratification, allowing for the simulation of both convective and stable regimes, including cloud formation and an accurate representation of the wind. Subgrid turbulence uses an anisotropic minimum dissipation model (7).

Terrain is represented using an immersed boundary technique, with the land-air interface modelled in detail including time and location dependent heat and moisture fluxes. Several global datasets are used as inputs to the model and are prepared in a pre-processing step. The orography is by default taken from the recent, 30m resolution Ensemble Digital Terrain Model (8). The ESA World-cover land-use map (9) is used to characterize the surface by setting a land-use dependent surface roughness length (z_0), as well as parameters for the TESSEL surface scheme, similar to that used in the global weather model by ECMWF(10). All flow-field arrays and time integration run on GPU, allowing domains >100 km with 100 m grid spacing and second-level temporal resolution.

2.2 Nested modeling framework

To adequately capture both synoptic-scale atmospheric variability and fine-scale turbulence in complex environments, a nested modeling framework is employed (See Fig. 1 for an overview). ERA5 reanalysis data, with a horizontal resolution of approximately 30 km, provide the large-scale meteorological boundary and initial conditions, ensuring consistency with the observed atmospheric state. The first downscaling step uses a 256 x 256 km meso-scale nest with 2 km resolution, which resolves regional weather patterns, land-sea heterogeneity and orographic effects. This is further refined to a 19.2 x 19.2 km domain with a turbulence-resolving resolution of 100 x 100 x 25 m. Here Large-Eddy Simulation (LES100) becomes appropriate, allowing explicit resolution of the dominant turbulent eddies. Turbulence perturbations are added at the boundaries of the LES to switch from modelled to resolved turbulence at the interface of the meso and LES100. These perturbations are temporally and spatially dependent to be consistent with the mesoscale inflow conditions, and are derived from a concurrent, periodic LES precursor. A final nest at 40 x 40 x 10 m resolution (LES40) is then introduced to capture canopy-scale flows and the influence of complex terrain features in detail.

2.3 Canopy representation

Within LES40, the vertical resolution explicitly resolves tree canopies and their direct influence on the flow. At coarser resolutions where individual trees cannot be represented, their aerodynamic effects are parameterized through height displacement and roughness length at 70% of the canopy height (11), ensuring consistent canopy-induced drag and turbulence production across scales. The LES approach at these finest scales is essential, as mesoscale turbulence parameterizations are insufficient to capture turbulence generation and momentum exchange in vegetated, heterogeneous landscapes. The combination of ERA5 forcing, meso-scale downscaling, and LES provides a robust multi-scale framework linking large-scale dynamics to local flow.

2.3.1 High resolution terrain data Accurate canopy modeling in complex terrain requires high-resolution terrain and forest data, as tree canopy heights can vary on spatial scales of ∼1 m, and are strongly time dependent due to natural growth, forestry management and commercial felling. The digital terrain map (DTM) represents ground elevation, the digital surface map (DSM) represents obstacle heights, and the canopy height map (CHM) represents tree heights. Airborne laser scanning (ALS) provides high-accuracy representations of tree tops and surfaces, but coverage is limited, so we developed a method to load local, high-resolution data sets, that are gap filled and extended using global datasets: AW3D30 DSM at 30 m (12), the global

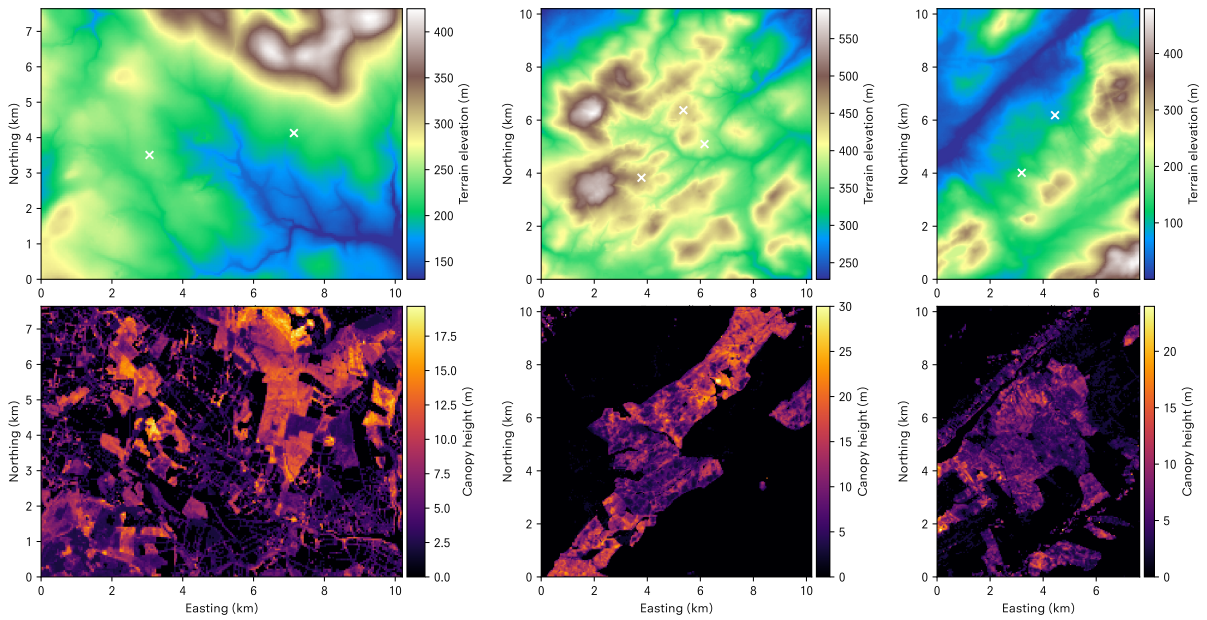

Figure 2: Overview of the three validation sites with on the top the terrain elevation map (DTM), and on the bottom the canopy height map (CHM). The location of the met masts is marked with a white cross.

ensemble DTM (8), and a 1 m CHM derived from Sentinel-2 and supervised by ALS and GEDI data (13). These datasets are carefully aligned and interpolated directly to the simulation grid in a single step, minimizing discontinuities and aliasing (Fig. 2). The transition between the datasets looks smooth, with similar canopy height and tree cover inside and outside the region with ALS data availability.

To maintain scale-independent canopy representation, canopy heights are averaged over grid points classified as trees, avoiding contamination from low vegetation, bare ground, or built-up areas. In ALS data, obstacles 2–50 m tall are treated as trees, as there are no major cities in the neighborhood and the resolution is high enough to mask individual trees. For larger domains, the 1 m CHM is coarse-grained and rescaled with the tree cover to recover mean canopy height at every resolution, while ALS domains are masked to prevent filling grid points with zero tree height. This also produces fractional tree cover per grid cell, allowing smooth scaling of canopy forcing. If the canopy height is lower than the first model layer, the tree forcing is represented by a canopy height-dependent roughness length at a height displacement of 70% of the canopy height (11). The resulting canopy forcing is therefore much smoother, especially on the edges of forests, and includes additional roughness elements in grid boxes that do contain, but are not dominated by trees (see the LES40 panel in Fig. 1).

2.4 Used metrics

To evaluate the performance of the simulation setup, we used the Mean Absolute Percentage Error over the wind direction sectors (MAPE), and its wind-direction-weighted counterpart. Observations with a wind speed <3 m/s are ignored in these statistics, as they are ill-defined, and irrelevant in wind resource assessment. MAPE quantifies the average magnitude of error in relative terms. Comparing relative metrics is easier for multiple sites, since the wind conditions can differ significantly from site to site. Since wind direction frequency plays a critical role in

wind resource assessment and cross-predictions over a site, given orography and time dependent variation in wind speed ratios over the field, we also applied wind-direction-weighted versions of these metrics.

2.5 Day selection

In general, real-weather LES comes at a substantial computational cost, because of the large range of spatio-temporal scales that are simulated. Therefore, limiting the run time while preserving the required output characteristics and accuracy is a crucial step in a cost-effective modeling setup. Since we focus in this project specifically on cross-prediction over sites, which is highly dependent on the wind direction in complex terrain, we devised a new day selection routine. The requirements for the chosen days are as follows:

1. They have to be representative of the long term wind speed distribution.
2. They have to result in a uniform wind direction distribution.
3. They should counter any risk on seasonal bias

Together these three points ensure that the metrics are converged, so that they are representative of the full measurement period, and that every wind direction has enough sample points so that cross-prediction for all wind direction sectors has a statistically significant result.

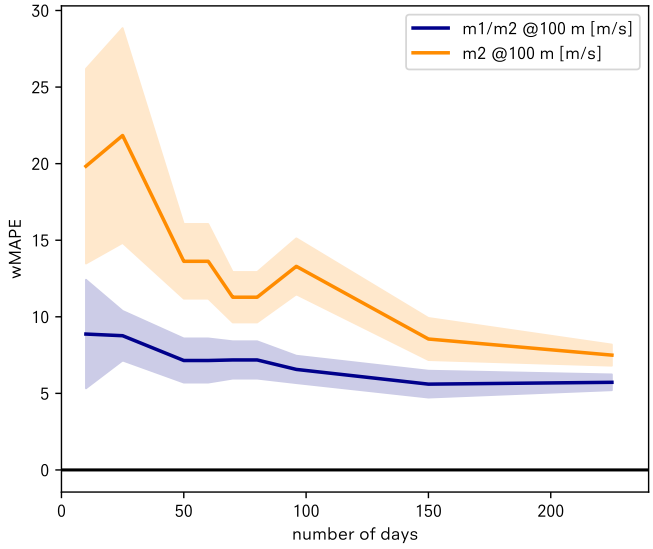

Figure 3: wMAPE as function of the chosen number of days for the wind speed ratio over the two metmasts at one of the test locations (blue), and the absolute wind speed at one of the met masts (orange). The line denotes the mean of 7 draws with a different random seed, and the errorbar shows the spread around the mean.

The day selection is done based on measurement data to maximize measurement availability over the simulated days and facilitate validation. The representative wind speed at any time is taken as the mean over the different mast and/or LiDAR locations and heights. As representative wind direction, we choose the location with the highest availability. Every date in the measurement data is represented as a 10-minute distribution, with 1 m/s bins in wind speed and 16 wind direction sectors. We measure time of year by dividing dates into monthly bins. Each date is assigned based on its position within the month: days near the middle of the month fall entirely into that month's bin, while days at the edges are split between adjacent months. To guide the random day selection process, we decided to pre-bin days in wind direction bins, based on the prevalent wind direction of the day. After pre-processing this data, we chose a high number of random drawings with the set number of days, and compare the mean of their

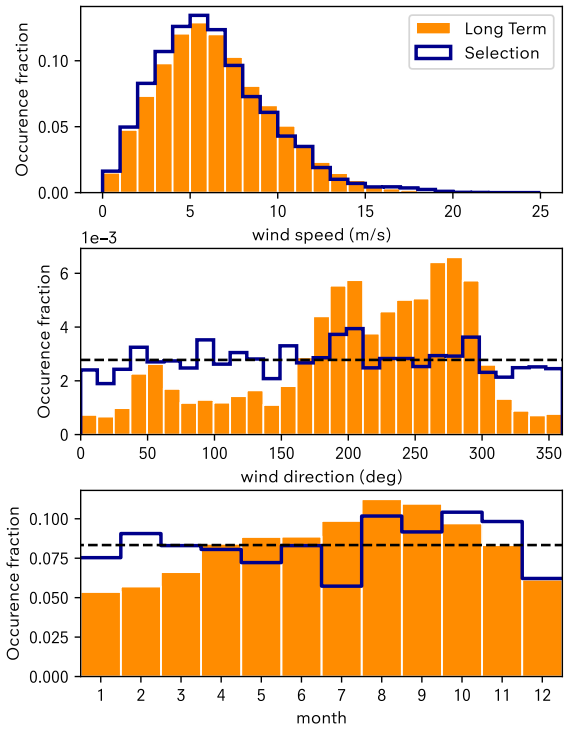

Figure 4: Wind speed, wind direction and monthly distribution for one of the test sites, showing the long term distribution (orange) and the distribution of the chosen 96 days.

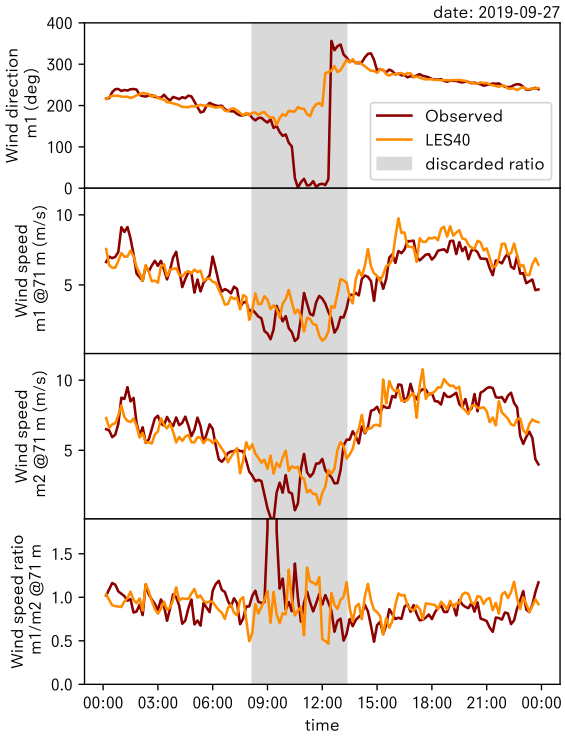

Figure 5: Time series of the wind direction, wind speed and the wind speed cross-prediction for M2 and M1.

distributions with the target distribution (mean of the long term wind speed, uniform wind direction and month) using the Perkins skill score (PSS)

$$\mathrm{PSS} = \sum_i \mathrm{minimum}(f(i), g(i)), \tag{1}$$

with f and g the input and target distribution, normalized to 1.

To decide on the number of days, we ran a long term (300 day) simulation on one of the sites and determined the skill compared to the long term simulation. The sub-selection is done seven times for a different number of days, $\{16, 32, 48, 64, 80, 96, 144, 256\}$, each with a different random seed. In Fig. 3, we show the mean and the standard deviation of the wMAPE as function of the chosen number of days, using a uniform distribution in wind direction. The metrics for the wind speed ratio converge to a consistent mean and spread after about 96 days. The wMAPE of the absolute wind speed prediction at the met mast is then past the logarithmic improvements as well. Considering that the distribution of wind speed and direction does not improve going to more than 70 days, we settle on a number of 96 days for every simulation.

2.6 WaSP setup for comparison

For all three validation sites, The WAsP linear flow model, developed by DTU, was used as a baseline to quantify cross-prediction errors between measurement locations and to enable a like-for-like comparison against the LES40 results reported in this study.

WAsP was configured using standard orographic and surface descriptions for each site. A digital terrain model (DTM) was used to represent elevation and slope effects, and a roughness map was prepared to describe spatial variations in surface drag (e.g., open land, moorland, forested areas). Forestry mapping was additionally used to derive a displacement height representative of the canopy influence at the mast location, ensuring that the initiation conditions reflect the effective zero-plane displacement in forested flow. These inputs were used to compute direction-dependent speed-up effects between the reference (initiation) mast and the secondary measurement location.

Unlike Whiffle's real-weather LES approach, WAsP requires on-site measurements to define the wind climate that drives the flow solution. A frequency distribution ("tab") file was generated from the reference measurement device to describe the long-term wind climate in terms of wind direction sector occurrence and wind speed distribution. WAsP then applies its linearized flow model to estimate the sector-wise speed-up factor between the initiation mast and the target location, accounting for the influence of terrain and roughness transitions embedded in the input maps. The resulting cross-predicted wind speed at the secondary location can be expressed as the reference wind speed multiplied by the modelled sector-dependent speed-up factor.

Model performance was assessed by comparing (i) the WAsP -predicted wind speed ratio between locations against (ii) the observed ratio from concurrent measurements and (iii) the corresponding LES40-derived ratio. In this way, differences can be attributed directly to the modelled flow modification between the two locations rather than to differences in the driving wind climate definition.

3 Validation results for relevant sites

Validation is performed on three different sites in Ireland and the United Kingdom, with complex terrain and forestry. In Fig. 2) we present an overview of each of the sites with the terrain elevation map and canopy height in the LES40 simulation.

3.1 Site overview

Test site 1 is located on forested land surrounded by moorland, characterised by thick grass, heather, and peaty terrain. Elevations range from sea level in the northwest to ∼450 m a.s.l. in the southeast. Measurements are taken using a meteorological mast and a LiDAR, positioned approximately halfway down the slope within a forested area. Forestry canopy heights range from ∼5 m to 25 m, with the majority of vegetation between 10 – 15 m.

Test site 2 has elevations ranging from ∼230 m to 600 m a.s.l., with two prominent hills near the centre of the domain. Ground cover is dominated by commercial forestry, forming a narrow strip across the site from southwest to northeast, with relatively high canopy heights up to ∼25 m. Measurements are taken at three locations; however, to avoid presenting degenerate cross-predictions, only the mast pairs (M1, M2) and (M3, M2) are shown.

Test site 3 features moderately complex terrain with elevations ranging from 140 m to 400 m a.s.l. A prominent valley runs through the domain, with a ridge towards the north. Ground cover consists of farmland and large areas of commercial forestry. Measurements are taken using meteorological masts on either side of the valley. The forest extends across the full LES40 domain, but canopy heights are relatively low across most of the area.

3.2 General validation

In this section we will illustrate the general accuracy of the simulations and how well different trends are captured.

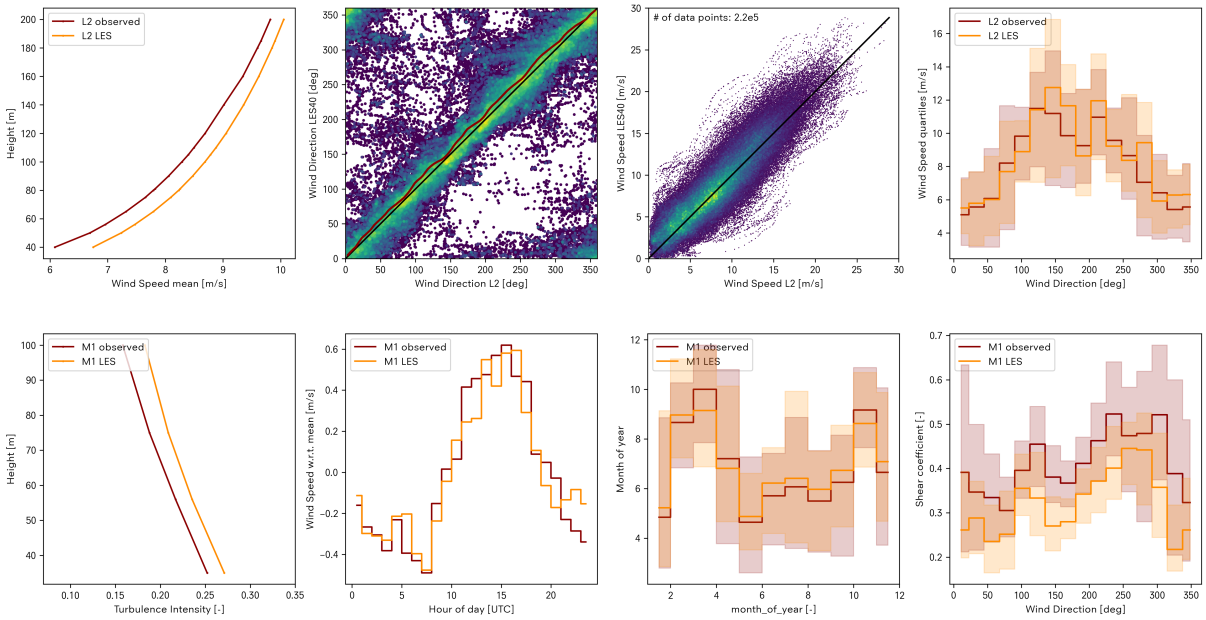

Figure 6: Typical skill of the simulations, Test site 1 is taken as an example. Top row from left to right: average vertical wind profile for L2 (red) and LES40 (orange). Quantile-quantile plot for the LES40 simulation versus observed wind direction at L2. Skill summary of the simulated LES40 versus observed wind speed. Wind speed as function of wind direction at L2. Bottom row from left to right: vertical profile of turbulence intensity at M1. Wind speed as function of hour of day at M1. Wind speed as function of month of year at M1. Shear coefficient as function of wind direction at M1. Shaded regions denote quartiles of the occurrence in the time series.

3.2.1 Day selection In Fig. 4 we present the wind speed, wind direction and seasonal distribution of the 96 days that are simulated for one of the test sites as an example. By design of the day selection algorithm, the wind direction and seasonality have a flat distribution, while the wind speed preserves the long term distribution. Even though the wind speed per wind direction bin is not ensured to be long-term represented, average quantities will have a high number of statistics in every wind direction bin, represent all seasons equally and will have the correct underlying wind speed distribution.

3.3 Wind speed cross-prediction

3.3.1 Typical skill and output In Fig. 5 we present a typical 10 minute averaged time series output of the model, compared with the observations. On the simulated day, September 27th 2019, a front passed at test site, resulting in an abrupt change of wind direction and varying wind speeds from 1 to 10 m/s. Both the LES100, and the LES40 simulation pick up this trend accurately, while also matching the absolute wind speed and direction. Any further results are derived from either point-wise or field time series. Note that wind speed ratios are discarded if either of the locations has observed wind speeds less than 3 m/s to avoid increased uncertainty by dividing through small numbers (masked region in Fig. 5).

A full-physics LES consistently and realistically captures trends in all relevant atmospheric variables. To demonstrate this, Fig. 6 shows the typical accuracy of various simulated quantities at Test site 1. The average vertical profile of wind speed and turbulence intensity is close to

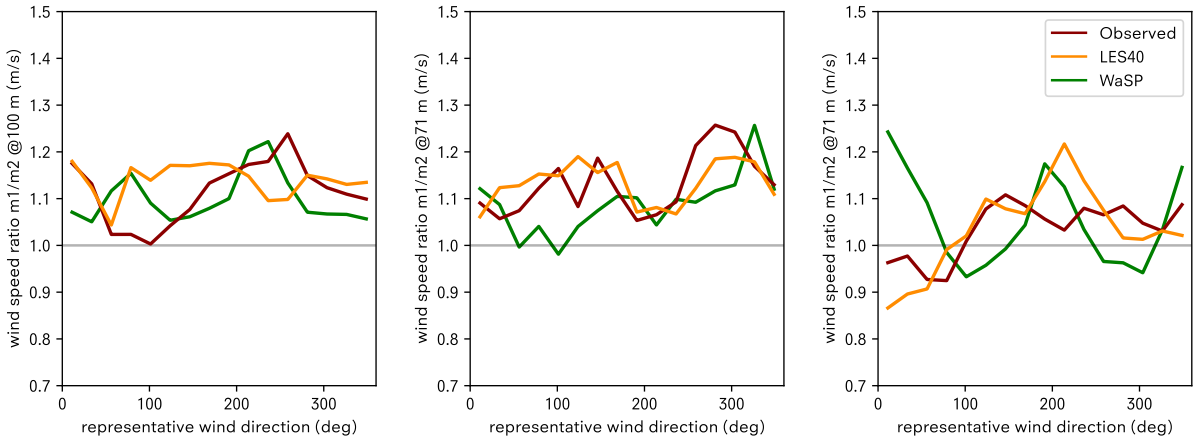

Figure 7: Wind speed cross-prediction at Test site 1, Test site 2 and Test site 3, as function of the wind direction for the observations (red), LES40 (orange), and a default WAsP setup (green).

reality, with an absolute bias of 0.4 m/s in wind speed in the LES40 simulation. The resulting wind direction in the LES40 simulation follows the one-to-one line with the observations, with an absolute deviation of $\sim 6^{o}$. Trends as functions of hour of day (due to the diurnal cycle of the sun), month of year (seasonal variations), and wind direction (orography, site heterogeneity) are well captured, both in terms of the absolute wind speed as well as the power law shear coefficient.

3.3.2 Typical skill The cross-prediction over each site, binned by wind direction is shown in Fig. 7, together with the observations. The strongest deviations from a wind speed ratio of 1 are a result of the complex orography on the sites. In addition, the flow fields of some characteristic wind directions are shown in Fig. 8 for Test site 1. Measurement locations that are behind a ridge, as seen from the flow direction, typically show higher wind speeds. Compare for example northerly winds at Test site 3 (M2 closer to the hills; wind speed ratio M1/M2 < 1) with south-westerly winds (M1 closer to the hills; wind speed ratio M1/M2 > 1).

The skill on the wind speed cross-prediction per site is summarized in Fig. 9. Overall, all sites are well represented in the model, with a typical MAPE of 3 – 5% and a wMAPE of 3 – 6%, which is a significant improvement compared to the WaSP result (6 – 12 and 5 – 10% for MAPE and wMAPE, respectively).

3.3.3 Future improvements In general, the observed trends with wind direction are picked up by the simulations (see Fig. 7), but in some sectors the speedup is over-predicted. On these complex sites, differences can be a result of many local details. Average wind speeds vary up to a factor of 2 over the sites, and a slightly wrong position of the (virtual) met mast, a hill side slightly offset on sub-pixel scales, a forest zone that is cut down etc. could all result in inaccuracy of the simulated wind speedup ratio. In addition, like every numerical model, LES also comes with its uncertainties and imperfections, which especially become prominent in the deviations from the observations as seen if one of the metmasts is just behind a hill top. For example, for Test site 1 the wind speed at M1 in the south-easterly sector is overestimated, for Test site 3, the wind speed at M1 in the south-westerly sector is overestimated, for Test site 2 the wind speed at M2 for north-westerly winds is overestimated. The most likely explanation

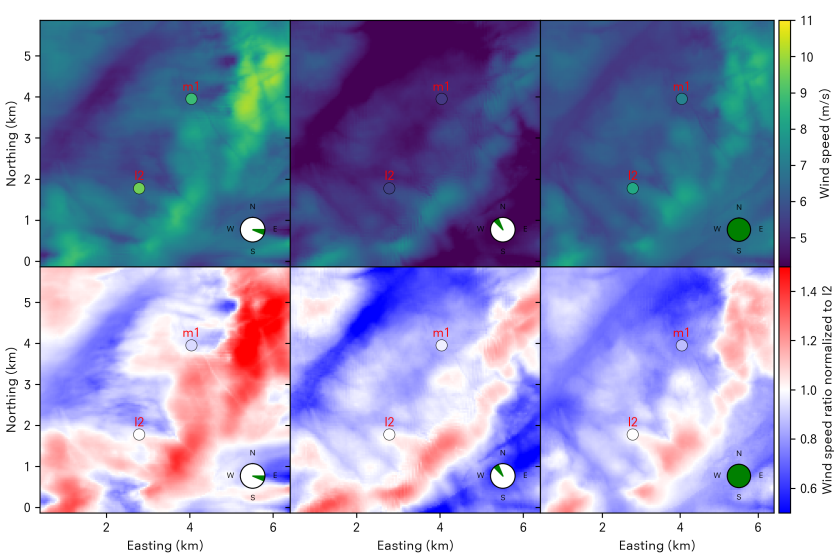

Figure 8: Average wind field at 100 m height for all instances with eastern (left), north-western (middle), and all wind directions at Test site 1. The top row shows absolute wind speeds, the bottom row shows wind speed relative to L2. Observations are color coded accordingly for visual comparison. Notice the strong gradients over the field and the absolute scale differences.

is an overprediction in wind speed at 100 m due to too much flow separation as a result of the numerical implementation of the terrain. Currently, the terrain is discretized onto the grid leading to a jagged representation of the terrain which promotes flow separation and increased turbulence. Work is currently ongoing at Whiffle to implement a smooth terrain representation in the LES.

4 Costs

Modeling complex terrain, and especially trees, requires a high resolution simulation grid in both horizontal and vertical directions. Running the full LES domain at 40 m instead of our default 100 m resolution requires a factor 2.5^3, $\sim$16, more cells. With the triple-nested setup, we limit the region of the high resolution grid both vertically and horizontally, while preserving the total domain size of the simulation necessary to capture the weather at all relevant scales.

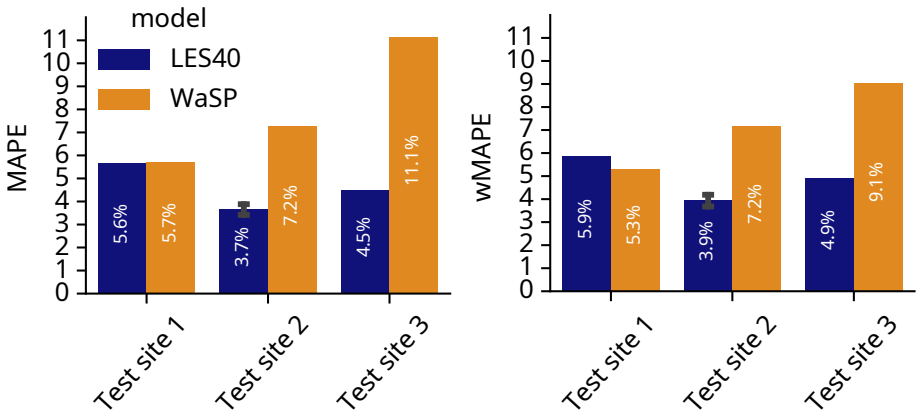

Figure 9: Overview of the wind speed ratio skill in LES40 across the three sites, evaluated using the four metrics described in Sect. 2.4. The spread over the multiple baselines at Test site 2 is marked with a black line.

The number of cells at high resolution is therefore on average only a factor 1.5 higher (1.6, 1.4, 1.2 for the three test sites, respectively) than in the parent LES. Using higher resolution grids also results in smaller simulation time steps, because the relevant time scale for the flow scales linearly with the resolution. The total runtime per day is therefore about a factor 4 higher than the LES100 alone. The smart day selection developed during the project and described in Sect. 2.5, results in a more cost-effective number of days with reliable results. Using this novel day selection recipe, we are able to cut the required number of days to 96.

5 Conclusions and outlook

A cost-effective simulation recipe was developed for optimized modelling of complex, forested sites in Whiffle's atmospheric LES framework. This approach led to the following concrete model and recipe improvements:

1. Cost-effective triple-nest setup, allowing to capture large-scale weather and local orography and forestry in one model, with limited additional run costs.
2. Whiffle's preprocessing engine was extended for seamless ingestion of high resolution DTM, DSM or CHM data into Whiffle LES.
3. Improvements were made in grid alignment and reprojection of geo-spatial data, leading to more accurate representation of terrain and forestry on all resolutions.
4. More consistent handling of CHM data, decoupling it from the DSM and DTM to allow for flexible masking and resolution-independent modelling of the tree canopy.
5. Coarse-graining and ingestion of an improved global canopy height dataset.
6. Improved canopy representation, with consistent scaling of tree cover and height.
7. Improved day selection, taking a uniform distribution of wind directions, while enforcing seasonality and the wind speed distribution to be represented correctly, allowing to cut the required number of days from 365 to 96 days.

The simulation recipe was validated at three relevant sites, showing absolute sectorial cross prediction errors of 3 to 5%, which is a significant reduction compared to the WaSP output (6 – 12 %). In addition to cross prediction, the model was shown to accurately capture absolute wind, turbulence and shear, as well as the sectorial, diurnal and seasonal trends.

The main discrepancies between the model and observations were found for sectors with strong downhill flow, attributed to too strong flow separation in the LES. Future work will focus on incorporating an improved terrain representation in the LES and test how this can further enhance the accuracy of cross predictions in complex terrain.

References

[1] Heus T, van Heerwaarden C C, Jonker H J J, Pier Siebesma A, Axelsen S, van den Dries K, Geoffroy O, Moene A F, Pino D, de Roode S R and Vilà-Guerau de Arellano J 2010 *Geosci. Model Dev.* **3** 415–444 ISSN 1991-959X, 1991-9603
[2] Neggers R A J, Siebesma A P and Heus T 2012 *Bulletin of the American Meteorological Society* **93**(9) 1389–1400 ISSN 00030007
[3] Schalkwijk J, Griffith E J, Post F H and Jonker H J J 2012 *Bulletin of the American Meteorological Society* **93**(3) 307–314
[4] Böing S J, Jonker H J J, Siebesma A P and Grabowski W W 2012 *Journal of the Atmospheric Sciences* **69**(9) 2682–2698 cited By 14
[5] Baas P, Verzijlbergh R, van Dorp P and Jonker H 2023 *Wind Energy Science* **8** 787–805

[6] Postema B, Verzijlbergh R A, van Dorp P, Baas P and Jonker H J J 2025 *Wind Energy Science* **10** 1471–1484
[7] Rozema W, Bae H J, Moin P and Verstappen R 2015 *Physics of Fluids* **27** ISSN 10897666
[8] HO Y F, Hengl T and Parente L 2023 Ensemble digital terrain model (edtm) of the world
[9] Zanaga D, Van De Kerchove R, Daems D, De Keersmaecker W, Brockmann C, Kirches G, Wevers J, Cartus O, Santoro M, Fritz S, Lesiv M, Herold M, Tsendbazar N E, Xu P, Ramoino F and Arino O 2021 ESA WorldCover 10 m 2021 v200
[10] Muñoz Sabater J 2019 ERA5-Land hourly data from 1950 to present. copernicus climate change service (C3S) climate data store (CDS)
[11] Floors R, Enevoldsen P, Davis N, Arnqvist J and Dellwik E 2018 *Wind Energy Science* **3** 353–370
[12] Takaku J, Tadono T, Doutsu M, Ohgushi F and Kai H 2020 *International Archives of the Photogrammetry, Remote Sensing and Spatial Information Sciences (ISPRS Archives)* **XLIII-B4** 183–189
[13] Tolan J, Yang H I, Nosarzewski B, Couairon G, Vo H V, Brandt J, Spore J, Majumdar S, Haziza D, Vamaraju J, Moutakanni T, Bojanowski P, Johns T, White B, Tiecke T and Couprie C 2024 *Remote Sensing of Environment* **300** 113888 ISSN 0034-4257